ISBN: 978-3-95450-212-7 ISSN: 2673-5482 doi:10.18429/JACoW-CYCLOTRONS2022-THPO013

MAGNET DESIGN OF A COMPACT 16 MeV VARIABLE ENERGY CYCLOTRON FOR ISOTOPE PRODUCTION

S. W. Xu, W. W. Wang, Hefei CAS Ion Medical and Technical Devices Co., Ltd., Hefei, China
K. Z. Ding, J. Zhou, F. Jiang, Z. Wu
Institute of Plasma Physics, Chinese Academy of Sciences, Hefei, China

Abstract

A compact isochronous cyclotron, CIMV16, is under research and development at Hefei CAS Ion Medical and Technical Devices Co., Ltd, China (HFCIM). This cyclotron can accelerate negative hydrogen ion to variable energy in the range of 10~16 MeV for the stable production of widely-used medical isotopes in this energy range. It has a maximal diameter of only 1.8 m and adopts three radial-sector poles with the third harmonic acceleration. The design of magnet system and the analysis of final simulated static magnetic field were described in detail in this paper. Meanwhile, two suitable shimming methods were also proposed for later engineering optimization.

INTRODUCTION

To meet the explosive growth of domestic health needs, China is actively producing medical radioisotopes. Important among them are ^{11}C, ^{13}N, ^{15}O, ^{18}F, etc. for PET (Positron Emission Tomography) and ^{64}Cu, ^{67}Ga, ^{86}Y, ^{124}I, ^{225}Ac, etc. for other medical applications, all of which require proton energy in the range of 10~16 MeV to yield them through nuclear reactions [1]. Due to the advantages of producing isotopes with high specific activity and less radioactive waste, the cyclotron has gradually become a critical option for the production of short-lived radioisotopes [2].

A cyclotron with a single extraction energy could not be suitable for producing various isotopes efficiently, so a variable-energy cyclotron that can simultaneously produce several isotopes is more adopted to the market demand. Internationally, the existing variable-energy cyclotrons below 20 MeV are TR-19, BEST 35p, CYCLONE 30, CC-18/9M, and so on [2]. However, in China, only a few cyclotrons with single-energy are available, such as CY-CIAE-14 from China institute of atomic energy (CIAE) [3]. For these reasons, HFCIM is developing a variable-energy cyclotron, CIMV16. To improve the extraction efficiency, it accelerates negative hydrogen (H^-) ion and extracts them by stripping foil, which can produce more than 100 μA protons with energies of 10~16 MeV, satisfying the production of the important isotopes described above.

The design of magnet system is the primacy of CIMV16. After the initial determine of magnet system parameters, the poles are further optimized according to the isochronous requirements. Then, the beam dynamics analysis is performed for a single particle, and the position of stripping foil is adjusted so that this particle can be extracted to a same focus point at different energies, which finally confirms that the magnet system meets our design requirements.

STRUCTURE DESIGN

The preliminary design of CIMV16 is based on the following assumptions:

- Primarily accelerates H^- ion.
- Isochronous cyclotron.
- Maximal extraction energy is 16 MeV.
- Isochronous field at $R = 0$ (B_0) is about 1.55 T.
- Axial betatron frequency (ν_z) is in the range of $0.10 < \nu_z < 0.25$ (beyond the central region).
- Radial-sector poles (spiral angle $\mu = 0$).
- Make enough space for RF system, and decrease RF voltage as much as possible.

Based on the above assumptions, The relativistic mass factor of H^- ion at maximal energy is expressed as $\gamma = (E_0 + E_k) / E_0 \approx 1.017$ (where E_0 is the rest energy 939.278 MeV and E_k is the maximal kinetic energy 16 MeV). Isochronism requires the maximal averaged field is calculated as $\langle B_e \rangle = \gamma B_0 \approx 1.58$ T. Therefore, the final orbit radius of particle (R_e) is estimated as 36.8 cm. Considering the magnetic field weakens so quickly in the pole-edge region and its distribution does not meet the requirements of radial focusing and isochronism, so the radius of pole is a little larger than R_e.

The next step is to evaluate the axial and radial focusing characteristics. Referring to the calculation by H. L. Hagedoorn and N. F. Verster [4], the 2nd order approximate expansion of radial and axial betatron frequency (ν_r and ν_z) can be written as Eq. (1) and (2):

$$\nu_r^2 \approx 1 + k + \frac{3N^2}{(N^2-1)(N^2-4)} F(1+\tan^2\mu), \quad (1)$$

$$\nu_z^2 \approx -k + \frac{N^2}{N^2-1} F(1+2\tan^2\mu), \quad (2)$$

where N is the number of poles, μ is the spiral angle of pole, F is the field flutter ($F = \langle B^2\rangle / \langle B\rangle^2 - 1$) and k is the positive field index ($k = R / \langle B\rangle \times \mathrm{d}\langle B\rangle / \mathrm{d}R$) for each radius R. k approaches to 0 at the radius of maximal averaged field. In order to make the ν_z here close to 0.20 without spiral angle ($\mu = 0$), the minimal field flutter 3.6% for 3 poles or 3.8% for 4 poles is required at this radius. For providing sufficient space for the RF system and other systems and ensuring the enough axial focusing, the three radial-sector poles with third harmonic acceleration is finally adopted in CIMV16.

ISBN: 978-3-95450-212-7 ISSN: 2673-5482 doi:10.18429/JACoW-CYCLOTRONS2022-THPO013

The magnetic field in mid-plane is obtained by finite element analysis (FEA). After several iterations, this magnitude of magnetic field is provided by a combination of conventional coils, poles made of DT4 and yokes made of 10# steel. The preliminary selection of conventional coils and magnet parameters are listed in Table 1 respectively.

Table 1: Magnet System Preliminary Parameters

Parameter	Value
Cross section of coils	145 × 155 mm^2
Amperes × Turns	60000 A
Current density	266.96 A/cm^2
Number of poles	3
Max. radius of pole	420 mm
Height of pole	25 mm
Outer radius of yoke	900 mm
Hill gap / Valley gap	40 / 90 mm
Total height of magnet	900 mm
Central field	1.36 T
Max. averaged field	1.57 T

The 3D-model of magnet system is described in Fig. 1where the left is the external view and the right shows its lower part. The blue, red and yellow parts represent yokes, coils and poles respectively. Furthermore, the vertical cross-section of the half magnet is shown in Fig 2.

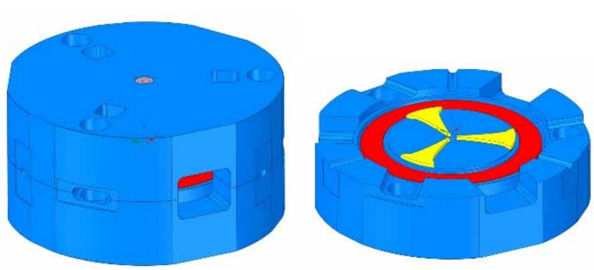

Figure 1: 3D-model of magnet system (left: external view; right: cross-section view).

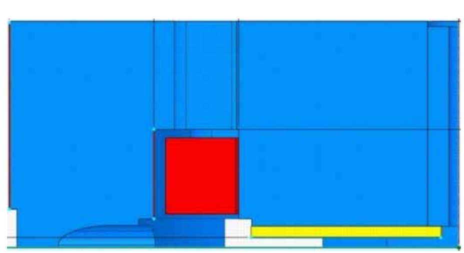

Figure 2: Vertical cross-section of magnet system.

ANALYSIS OF STATIC FIELD

After the initial parameters of the magnet system are determined, the average magnetic field in the mid-plane is gradually close to the isochronous one by optimizing the coil current, pole profile, and RF frequency according to isochronous requirements. A further model is obtained by considering both the magnetic field in the central region and the focusing properties in the extraction region, with the coil current eventually set to 60000 A and the RF frequency set as f_{RF} = 23.6 × 3 = 70.8 MHz. The static magnetic field simulated for this model is analysed below. Figure 3 depicts the comparison of averaged field (<B_z>) with isochronous one (B_{iso}). It can be seen that the <*Bz*> drops in the central and extraction region.

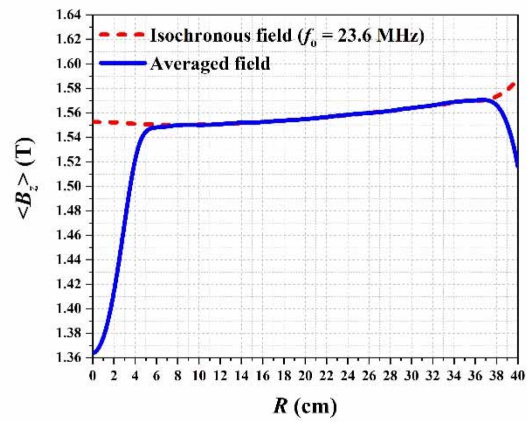

Figure 3: Comparison of averaged field (blue solid line) with isochronous field (red dash line).

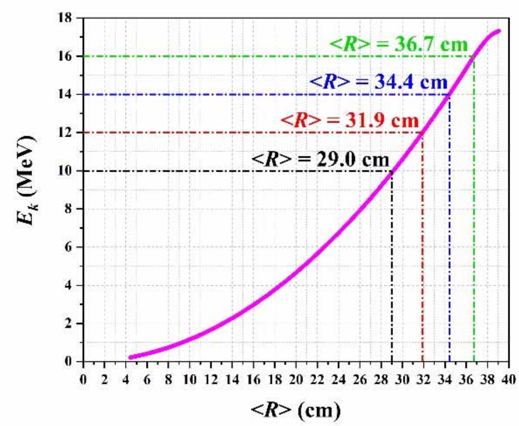

Figure 4: Relation between averaged radius and kinetic energy.

The relation between averaged radius (<*R*>) and kinetic energy (E_k) based on the static equilibrium orbit is shown in Fig. 4. Notably, 10, 12, 14, 16 extraction energy corresponds to 29.0, 31.9, 34.4, 36.7 cm averaged radius separately.

Figure 5 exhibits an important indicator of whether the isochronism is excellent: integral phase slip along the radius. The difference between averaged and isochronous field is also added in this figure. It is obvious that the difference between averaged and isochronous field has been controlled within ±10 G and integral phase slip has been controlled within ±10° less than 36.7 cm extraction averaged radius (16 MeV extraction energy).

The radial and axial betatron frequency (ν_r and ν_z) as shown in Fig. 6 can be also calculated from the static equilibrium orbit. As shown in this picture, sufficient axial focusing ($0.10 < \nu_z < 0.20$) is provided in the radial range

ISBN: 978-3-95450-212-7 ISSN: 2673-5482 doi:10.18429/JACoW-CYCLOTRONS2022-THPO013

more than 6 cm. Aside from this, the Walkinshaw resonance (ν_r / 2 = ν_z) has been avoided before the particle is accelerated to 16 MeV (corresponding to 36.7 cm). From the Fig. 7 work diagram, the particle does not cross any dangerous resonance lines except for a fast crossing of $\nu_r = 1$ at the end of acceleration, 15.9 MeV. Thus, the focusing satisfies the demands.

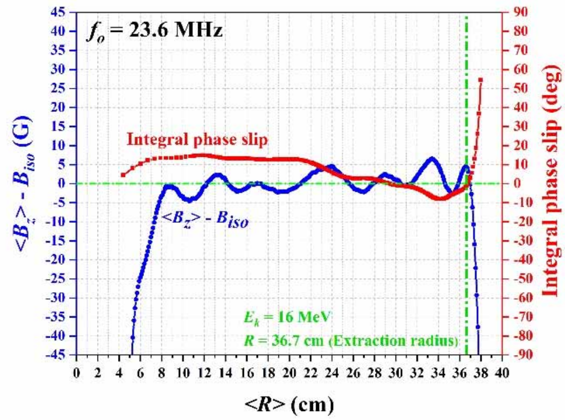

Figure 5: Difference between averaged and isochronous field (left axis); integral phase slip (right axis).

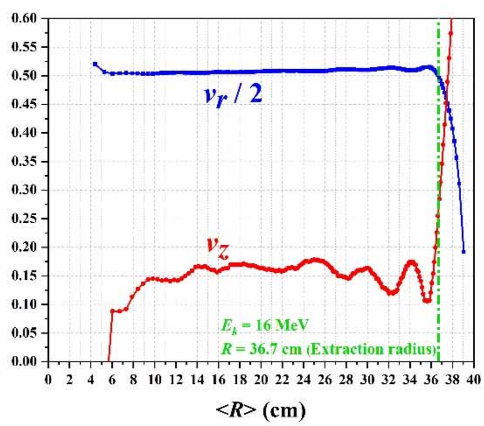

Figure 6: Radial and axial betatron frequency (ν_r and ν_z).

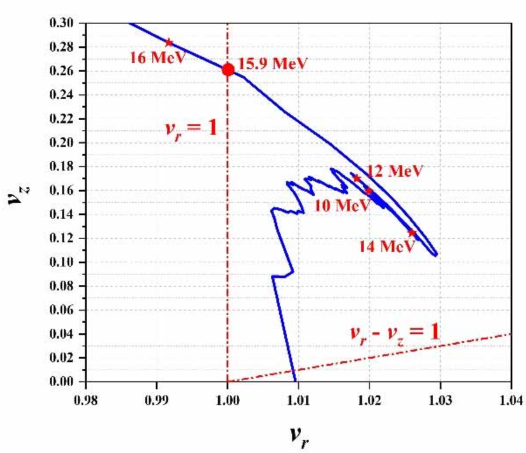

Figure 7: Work diagram.

DETERMINE OF EXTRACTION RADIUS

At last, to check whether the designed cyclotron can extract the beam at various energies successfully and to determine the location of extraction channels in the model of magnet system, the beam dynamics is performed for a single centre particle. Particle extraction energies of 10, 12, 14, 16 MeV are chosen and their beam trajectories are described in Fig. 8. H^- ion can be stripped out two electrons to become proton to be extracted by setting the stripping foils near the trajectories at the corresponding extraction energies. Via adjusting the radial and angular positions of the stripping foils (as summarized in Table 2), the protons with different energies can be extracted and intersect at the same point of around 110 cm. After this, the design of magnet system is completed.

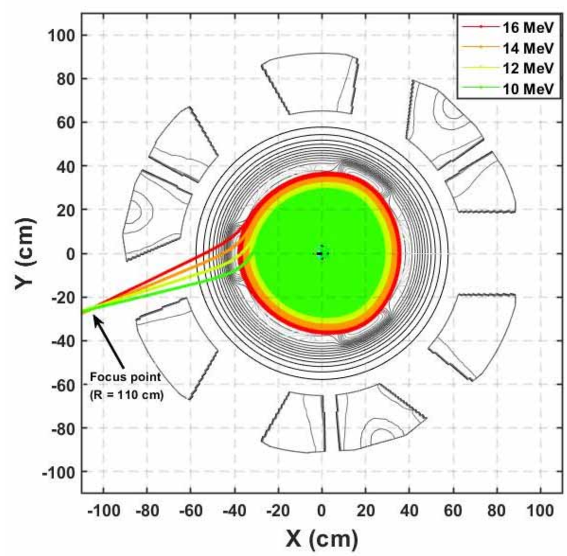

Figure 8: Trajectory of centre particle with different extraction energies.

Table 2: Parameters of magnet

Extraction Energy (MeV)	Stripping Foil Radius (cm)	Stripping Foil Angle (deg)
10	30.0	170
12	32.5	164
14	34.5	158
16	37.0	153

SHIMMING METHODS

Taking into account the poles shimming during the engineering phase, two methods are put forward as follows: The 1st is to fill the central groove (which is prepared in advance) at the surface of each pole; the 2nd is to cut the two laterals of poles. Their 3-D models are shown in Fig. 9.

For each method, a numerical algorithm expressed by J. Q. Zhong [5] can be used for calculating shimming value rapidly. For example, many shimming elements whose sizes are all 1 cm radius, 9 mm arc length, and 7 mm height are established along the radius for the 1st method, then

ISBN: 978-3-95450-212-7 ISSN: 2673-5482 doi:10.18429/JACoW-CYCLOTRONS2022-THPO013

their averaged field distributions along the radius are simulated by FEA, forming a matrix *F*. The result of them is depicted in Fig. 10. Assuming that the arc length of each element is expressed as a vector *X*, and vector *D* represents the required shimming field along the radius, then the *X* can be solved by least square method with the equation: $F \cdot X = D$. The same algorithm can be applied for the 2nd shimming method, where the size of each element is 1 cm radius, 3 mm arc length, and 25 mm height (the height of pole). Figure 11 shows the averaged field distributions along the radius of each element.

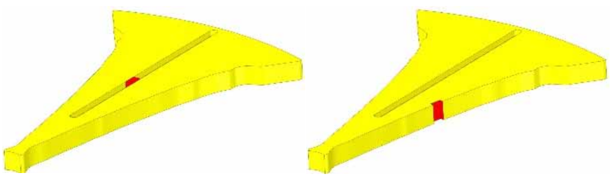

Figure 9: Two methods of poles shimming: to fill the central groove (left) and to cut the laterals (right). The red part is the shimming element.

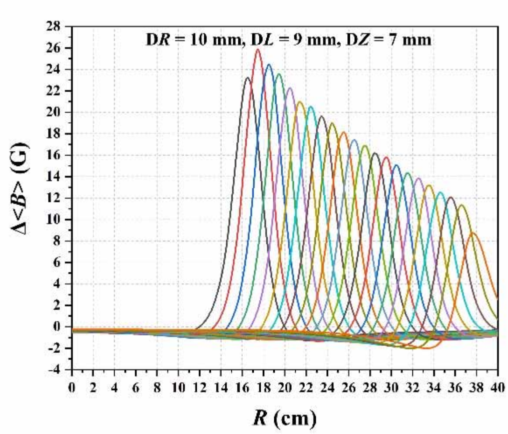

Figure 10: Averaged field distributions along the radius of each element for the 1st shimming method.

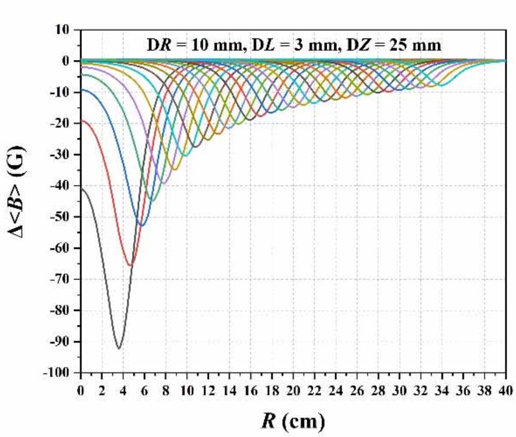

Figure 11: Averaged field distributions along the radius of each element for the 2nd shimming method.

CONCLUSION

This paper illustrates the process of designing the magnet system for a variable-energy cyclotron: CIM16V. Following the preliminary assumptions, it is confirmed that the three radial-sector poles with third harmonic acceleration is adopted for larger RF space. Also, the primary parameters of magnet system are determined. Then, about the final iterated model, analyses of the static magnetic field in mid-plane and the beam dynamics analyses of single particle result in the following conclusions:

- Difference between averaged and isochronous field has been controlled within ±10 G and integral phase slip has been controlled within ±10 deg.
- Sufficient axial focusing ($0.10 < \nu_z < 0.20$) is provided in the radial range more than 6 cm.
- The particle does not or does not slowly cross any dangerous resonance lines (rapidly cross $\nu_r = 1$)
- Realize the extraction of particle in the energy range of 10~16 MeV and make this particle with different energies intersect at a same focus point by the position adjustment of stripping foil.

After confirming that the design of magnet system is finished, two shimming methods of pole profile: to fill the central groove and to cut the laterals are proposed for the engineering optimization.

Currently, the design of other systems are in progress. HFCIM will finish the design and manufacture of this cyclotron as soon as possible to supply the isotopes for the domestic market, in particular the production of ^{18}F.

REFERENCES

[1] A. I. Papash and Yu. G. Alenitsky, “Commercial Cyclotrons. Part I Commercial Cyclotrons in the Energy Range 10-30 MeV for Isotope Production”, *Phys. Part. Nucl.*, vol. 39, no. 4, pp. 597–631, 2008. doi:10.1134/S1063779608040060

[2] P. Schmor, “Review of Cyclotrons for the Production of Radioactive”, *Rev. Accl. Sci. Tech.*, vol. 4, pp. 103–116, 2011. doi:10.1142/S1793626811000574

[3] T. J. Zhang *et al.*, “Overall design of CYCIAE-14, a 14 MeV PET cyclotron”, *Nucl. Instrum. Methods Phys. Res. Sect. B*, vol. 269, no. 24, pp. 2950-2954, Dec. 2011. doi:10.1016/j.nimb.2011.04.049

[4] H. L. Hagedoorn and N. F. Verster, “Orbits in an AVF Cyclotron”, *Nucl. Instrum. Methods*, vol. 18-19, pp. 201-228, 1962. doi:10.1016/S0029-554X(62)80032-9

[5] J. Q. Zhong *et al.*, “The physics design of magnet in 14 MeV cyclotron”, *Sci. Chin. Phys., Mech. Astron.*, vol. 54, no. S2, pp. 266–270, Dec. 2011. doi:10.1007/s11433-011-4551-2